Multi-Cell Interference Aware Resource Allocation for Half-Duplex Relay Based Cooperation

Cédric Abgrall[†‡], Emilio Calvanese Strinati[†] and Jean-Claude Belfiore[‡]
Email: cedric.abgrall@cea.fr, emilio.calvanese-strinati@cea.fr and jean-claude.belfiore@telecom-paristech.fr

[†] CEA, LETI, MINATEC
17, rue des Martyrs - 38054 Grenoble, France

[‡]TELECOM ParisTech (ENST)
46, rue Barrault - 75013 Paris, France

ABSTRACT

***Abstract*—The goal of our work is to limit inter-cell interference in two hops cooperative communication systems. We propose to exploit the standard half-duplex limitation of relays so as to coordinate in time and frequency the resource allocation of a cluster of neighbor cells, and then to adapt resource allocation to changes in the communication context. Simulation results show how our proposed allocation modes permit to outperform classical modes in terms of cooperation effectiveness, power consumption and perceived Quality of Service (QoS).**

I. INTRODUCTION

Nowadays, wireless networks target to improve capacity, extend coverage and limit energy wastage while meeting QoS constraints. With the growing number of users and the coexistence of different standards, available frequency resources become more and more scarce to ensure optimal orthogonal resource allocation between each transmission in the network. Radio frequency resources are shared, causing often prejudicial intra- and inter-cell interference.

Several methods have been investigated to cope with the interference issue. First, interference can be fought by efficiently allocating frequency and time resources to concurrent network agents. Full *time* and *frequency* orthogonal allocations consent to avoid inter- and intra-cell interference. However, such techniques impose stringent constraints on resource allocation algorithms. A more flexible approach is *Frequency Reuse* which basically consists in reallocating part of frequency resources in adjacent spatial locations [1]. The reuse of frequency resources can be either static or dynamic, with different resource assignments between cell-edge and cell-center users [1] [2]. Second, signal processing can help in coping with interference. Literature differentiates *Interference Avoidance* approaches (*e.g. Dirty Paper Coding* - DPC), from *Interference Cancelation* approaches (*e.g. Successive Interference Cancelation* - SIC). With DPC techniques, interference is pre-subtracted from intended message at the transmitter, which is assumed to have knowledge on it. Interference perceived at reception will then be cancelled out at reception [3]. With SIC techniques the receiver firstly decodes the strongest interfering signal, treating all other signals as noise, and then subtracts it. Iteratively, the process restarts with the second strongest interfering signal, and so forth until the wished message is decoded [3]. Additionally, several researchers proposed solutions based on *Interference Alignment* [4] [5]. Each system disposes of a limited amount of degrees of freedom. Some of them are 'sacrificed' to align interfering signals on them; the other degrees of freedom are eventually interference-free. Interference issue in a system can be settled by channel aware mechanisms, *e.g.* Power Control, Adaptive Modulation and Coding (AMC) [6]. Game theory, convex optimization and graph coloring are powerful and well-suited concepts [7] [8]: inter-cell interference is integrated into a utility function to optimize, taking into account local constraints; a well-known technique for Power Control is *Water-Filling* [9]. A more simple approach assigns either full or null power (*On-Off Power Allocation*) [10].

In this paper we focus on two hops cooperative based communications. Spatial diversity, coverage and transmission reliability can be enhanced by judicious cooperative techniques. Communications with relays may be particularly beneficial for cell-edge users, experiencing important path-loss attenuation and suffering from strong inter-cell interference. On the contrary, from a single link viewpoint, the addition of relays is not always the best solution: noise is amplified with AF strategy, whereas erroneous decoding is possible with DF [6]. Besides, from a system viewpoint, cooperation introduces additional interfering sources in the system: relays overlap the same sets of resources as those of sources ever active. Cooperation in wireless networks is like a crowded cocktail party with a cacophony of conversations all around. There is a trade-off between the level of interference and beneficial effects of cooperation. The more people repeat the same information, the more likely you understand it. However, repeaters introduce additional interference, which harms message understanding. The gains brought by cooperation of one relay should outperform the degradation that its activation may cause on neighbor cells.

Common assumptions in literature are the use of *half-duplex* relays, *i.e.*, relays cannot transmit and listen simultaneously. In case of OFDMA systems, relays can be *half-duplex per chunk*, *i.e.*, a relay is *half-duplex* for a given chunk but its behavior on each chunk is independent: relays are able to listen on a chunk while they are transmitting on another. A half-duplex per chunk aware Radio Resource Management (RRM) design is proposed here. Resource allocation is coordinated in neighbor cells, so as to prevent relays from suffering from too prejudicial inter-cell interference. Interfering transmissions

978-1-4244-2519-8/10/$26.00 ©2010 IEEE

are aligned on resources used by relays when they are 'deaf'. The cooperative interference-benefits trade-off is furthermore taking into account with adaptive techniques.

II. System Model and Notations

In this section, notations and system model adopted in the rest of the paper are introduced. The considered system is shown on Figure 1 and accounts of tri-sectorized cells of radius r_{cell}. Our analysis is focused on three adjacent sectors.

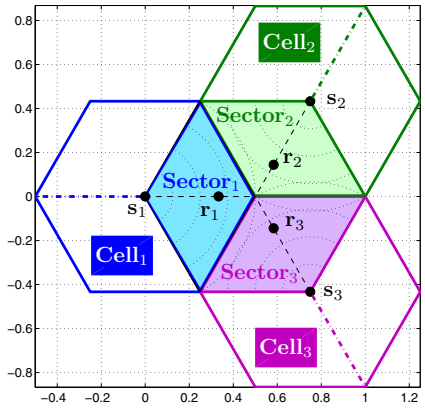

Fig. 1: System model with three adjacent sectors

Each sector, denoted by S_i, consists of a source $\mathbf{s}_i$ (base station for downlink transmissions), a single user equipment $\mathbf{d}_i$ as destination and a single relay station $\mathbf{r}_i$. Relays are fixed and all have the same location relative to their sector, at two thirds of r_{cell} from their base station, on the symmetry axis of the sector. All network agents are equipped with only one antenna. Relays work in half-duplex per chunk mode; they can be active or remain silent for a given transmission.

Each transmission can be done on maximum N_{chunks} frequency chunks. Channel gains and transmit powers are relative to a given chunk and are identified by the index of the chunk in exponent between brackets (omitted if referring to all chunks or if equality between chunks). Source $\mathbf{s}_i$ and relay $\mathbf{r}_i$ transmit respectively with powers $P_{s_i}^{(k)}$ and $P_{r_i}^{(k)}$ on chunk k. Channels between $\mathbf{s}_i$ and $\mathbf{d}_j$, $\mathbf{r}_i$ and $\mathbf{d}_j$, $\mathbf{s}_i$ and $\mathbf{r}_j$ are respectively denoted by coefficients $f_{ij}^{(k)}$, $g_{ij}^{(k)}$ and $h_{ij}^{(k)}$, on chunk k. These coefficients represent the global gain of channels, including fading, shadowing, path loss attenuation and AWGN noise. They remain constant during at least one frame transmission. Fading follows a Rayleigh distribution with unitary expectation. Log-normal shadowing is generated using the method described in [11]. Path loss model is the one of Okumura-Hata with $\text{PL}_{\text{dB}} = L + k.log_{10}(d)$ in dB, d [km] is the distance between transmitter and receiver. Transmitters are assumed to have perfect knowledge of all channel gains.

A schematic illustration of the two-hop channel model for one sector S_i is given on Figure 2. $\mathbf{d}_i$ and $\mathbf{r}_i$ are respectively subject to both noise (with variance $\sigma_{d_i}^2$ and $\sigma_{r_i}^2$), and inter-sector interference I_i and J_i. Relays can perform both ODF (*Orthogonal Decode and Forward*) or OAF (*Orthogonal Amplify and Forward*) protocols, *Orthogonal* since resources for transmissions of both hops are orthogonally allocated.

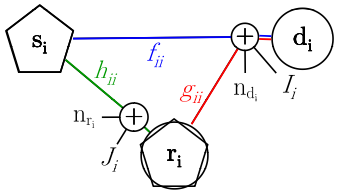

Fig. 2: System model for the set $\{\mathbf{s}_i,\mathbf{r}_i,\mathbf{d}_i\}$

III. RRM Designs Description

In our work, time and frequency resources are assigned to neighbor sectors according to three allocation strategies: *Classic*$_1$, *Classic*$_2$ and *Advanced*. For an easier explication, allocation designs are presented hereafter for only two frequency chunks ($N_{chunks} = 2$). No power control is done in a sector, while a simple on-off power allocation between sectors is applied to sources and relays. Indeed, sources and relays either do not transmit, or transmit respectively at power P_{s_i} and P_{r_i}. More chunks and any power control mechanisms can be combined to our examples.

Notation is the following. Each allocation pattern is labeled with three letters and an index. First letter refers to sector one (S_1), second to sector two (S_2) and third to sector three (S_3), while the index indicates the allocation strategy ('C1', 'C2' or 'A'). Each letter indicates either if in the *i-th* sector cooperation ('*C*') or no cooperation ('*N*') is planned. Indeed, 2^3 families of allocation modes are defined for each of the three strategies. Figures 3, 4 and 5 show the most representative allocation modes. Patterns are represented as follows: rows and columns are respectively divided into time slots and frequency chunks that can be either assigned to only one transmitter or shared (see for instance NNN_{C1} on Fig. 3a: the 2$^{\text{nd}}$ chunk is shared). Message index is given in exponent between brackets.

A. *Classic*$_1$ *Inter-Site Allocation Modes*

With *Classic*$_1$ RRM strategy, at a given scheduling moment, one chunk is granted one sector (S_1 for instance), while the other chunk is shared by the remainder two sectors (S_2 and S_3 for instance). Hence, one sector is advantaged in term of inter-sector interference. Therefore, in our examples, S_1 is interference free, while $\mathbf{d}_2$ and $\mathbf{d}_3$ are interfered by transmissions occurring respectively in S_3 and S_2. Expressions of channel capacity can be specifically derived for each allocation mode. When no sector plans cooperation (NNN_{C1}), mutual information amount $\mathscr{I}^i$ of sector S_i can be expressed as:

$$\begin{aligned} \mathscr{I}^1_{\text{NNN}_{\text{C1}}} &= \log_2\left(1 + P_{s_1}^{(1)}.f_{11}^{(1)}\right) \\ \mathscr{I}^i_{\text{NNN}_{\text{C1}}} &= \log_2\left(1 + \frac{P_{s_i}^{(2)}.f_{ii}^{(2)}}{1 + P_{s_j}^{(2)}.f_{ji}^{(2)}}\right) \\ i \neq j, (i,j) &= \{2,3\} \end{aligned} \tag{1}$$

Neighbor transmissions are synchronized: active transmitters ($\mathbf{s}_i$ or $\mathbf{r}_i$) in S_2 and S_3 simultaneously broadcast on the second chunk. If cooperation is planned in S_2 or S_3 (*i.e.,* on the 2$^{\text{nd}}$ chunk) (Fig. 3c–3f), relay listening phase is interfered by transmission of the neighbor source. Relays ought not to cooperate if the signal they listen to is too interfered. Most illustrative *Classic*$_1$ allocation modes are shown on Figure 3.

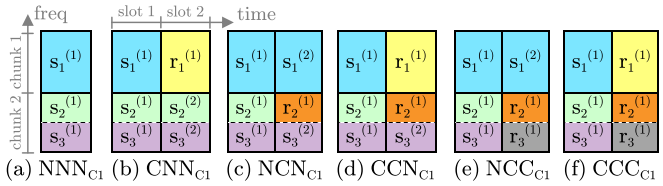

(a) NNN_{C1} (b) CNN_{C1} (c) NCN_{C1} (d) CCN_{C1} (e) NCC_{C1} (f) CCC_{C1}

Fig. 3: Allocation modes for *Classic*$_1$ strategy

B. *Classic*$_2$ Inter-Site Allocation Modes

With *Classic*$_2$ allocation modes, there is no frequency planning between sectors: both chunks are assigned to all sectors. Therefore, each destination suffers, on both chunks, from interference caused by neighbor active transmitters ($\mathbf{s}_i$ or $\mathbf{r}_i$). When cooperation is planned in a sector, relay listening phase is interfered by transmission of neighbor sources. In comparison to *Classic*$_1$ allocation modes, relays and destinations encounter more interference, but sources and relays transmit in return on both chunks.

Most illustrative modes are shown on Figure 4. Channel capacity of sector S_i for NNN_{C2} mode is derived as:

$$\begin{aligned}\mathscr{I}^{i}_{\text{NNN}_{\text{C2}}} &= \log_2\left(1+\frac{P^{(1)}_{s_i}.f^{(1)}_{ii}}{1+P^{(1)}_{s_j}.f^{(1)}_{ji}+P^{(1)}_{s_k}.f^{(1)}_{ki}}\right)\\ &+\log_2\left(1+\frac{P^{(2)}_{s_i}.f^{(2)}_{ii}}{1+P^{(2)}_{s_j}.f^{(2)}_{ji}+P^{(2)}_{s_k}.f^{(2)}_{ki}}\right)\\ &i\neq j\neq k,\quad (i,j,k)=\{1,2,3\}\end{aligned} \tag{2}$$

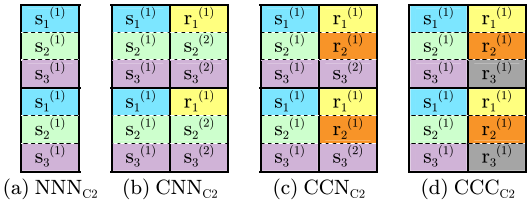

(a) NNN_{C2} (b) CNN_{C2} (c) CCN_{C2} (d) CCC_{C2}

Fig. 4: Allocation modes for *Classic*$_2$ strategy

C. *Proposed Advanced Inter-Site Allocation Modes*

This strategy of allocation modes is designed for half-duplex per chunk relays. Source $\mathbf{s}_i$ transmits on a chunk the packet m_k, relay $\mathbf{r}_i$ listens to m_k on this chunk while transmits the packet m_{k-1} on the other chunk. Transmission of one single packet always requires two time slots, but for n packets it needs $(n+1)$ time slots, which asymptotically tends to n. The allocation patterns which are investigated hereafter are thus reduced to one time slot (two time slots with classical strategies). When resource allocation is scheduled, one chunk is granted one source ($\mathbf{s}_1$ for instance), while remainder sources ($\mathbf{s}_2$ and $\mathbf{s}_3$ for instance) share the other chunk. Hence, one source is advantaged in term of inter-sector interference. Assume below that $\mathbf{s}_1$ is the advantaged source.

Destination $\mathbf{d}_1$ is interfered on the first chunk by neighbor relays, if S_2 or S_3 plans cooperation. Destinations $\mathbf{d}_2$ and $\mathbf{d}_3$ are interfered on the second chunk respectively by $\mathbf{s}_3$ and $\mathbf{s}_2$, and also by $\mathbf{r}_1$ if S_1 plans cooperation.

When no sector plans cooperation, NNN_{A} mode is defined as NNN_{C1} (Fig. 3a). If S_1 plans cooperation, $\mathbf{r}_1$'s listening phase on the first chunk is interfered by neighbor relays transmissions, only if S_2 or S_3 plans cooperation too (see Fig. 5a, 5c and 5e); on the other hand, $\mathbf{d}_1$ is always interfered by $\mathbf{s}_2$ and $\mathbf{s}_3$ on the second chunk. The amount of mutual information in sector S_1 for CNN_{A} mode is expressed, in case of OAF and ODF protocols [12], as:

$$\begin{aligned}\mathscr{I}^{1}_{\text{CNN}_{\text{A}},\text{AF}} &= \log_2\left(1+P^{(1)}_{s_1}.f^{(1)}_{11}\right)\\ &+ \log_2\left(1+\frac{P^{(1)}_{s_1}.h^{(1)}_{11}.P^{(2)}_{r_1}.g^{(2)}_{11}}{P^{(2)}_{r_1}.g^{(2)}_{11}+\left(1+P^{(1)}_{s_1}.h^{(1)}_{11}\right).X}\right)\\ \text{with } X &= 1+P^{(2)}_{s_2}.f^{(2)}_{21}+P^{(2)}_{s_3}.f^{(2)}_{31}\\ \\ \mathscr{I}^{1}_{\text{CNN}_{\text{A}},\text{DF}} &= \log_2\left(1+P^{(1)}_{s_1}.f^{(1)}_{11}\right)\\ &+ \log_2\left(1+\frac{P^{(2)}_{r_1}.g^{(2)}_{11}}{1+P^{(2)}_{s_2}.f^{(2)}_{21}+P^{(2)}_{s_3}.f^{(2)}_{31}}\right)\end{aligned} \tag{3}$$

If S_2 plans cooperation (likewise for S_3, by symmetry), $\mathbf{r}_2$'s listening phase on the second chunk is interfered by $\mathbf{s}_3$, and also by $\mathbf{r}_1$ if S_1 plans cooperation too; $\mathbf{d}_2$ is always interfered on the first chunk by $\mathbf{s}_1$, and also by $\mathbf{r}_3$ if S_3 plans cooperation. Most illustrative modes are shown on Figure 5.

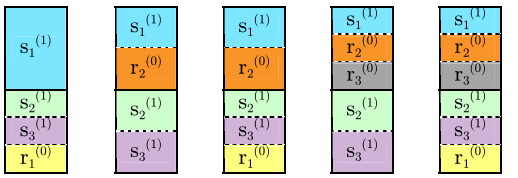

(a) CNN_{A} (b) NCN_{A} (c) CCN_{A} (d) NCC_{A} (e) CCC_{A}

Fig. 5: Allocation modes for *Advanced* strategy

IV. Algorithm for Adaptive RRM Design

Relay based transmissions in cooperative networks may improve channel capacity, but also enhance inter-sector interference and overall transmit power. Furthermore, an optimal allocation mode for a given communication context can be suboptimal with another context, since perceived inter-sector interference level is specific to each allocation mode. Therefore, in order to profit from time, frequency and space variations of communication context, without requiring excessive transmit power, an *Adaptive inter-sector Resource Allocation Process* (ARAP) is investigated.

Overall transmit power per allocation mode depends on the number and nature of transmitters as well as the number of chunks used by each transmitter. Given the transmission pattern, overall transmit power is easily defined. For instance, Table I expresses these power budgets, when all sources and respectively all relays transmit with equal powers.

Resources are adaptively assigned in accordance with one of the allocation modes introduced in Section III and in the interest of the overall system. Selection of the optimal mode is based on its Global Mutual Information (*GMI*) value and on its power budget, where *GMI* stands for the sum of mutual

	NNN	CNN,NCN,NNC	CCN,CNC,NCC	CCC
C1	$3.P_s$	$5.P_s$+P_r	$2(2.P_s$+$P_r)$	$3(P_s$+$P_r)$
C2	$6.P_s$	$2(5.P_s$+$P_r)$	$4(2.P_s$+$P_r)$	$6(P_s$+$P_r)$
A	$3.P_s$	$3.P_s$+P_r	$3.P_s$+$2.P_r$	$3(P_s$+$P_r)$

TABLE I: Overall transmit power per allocation mode, with equal powers P_s and P_r between sectors and chunks.

System model		Algorithm
$P_{s_i} = 10W$	$N_{chunks} = 2$	$N_{pos} = 1000$
$P_{r_i} = 1W$	$\sigma^2_{d_i} = \sigma^2_{r_i} = -105$dBm	$N_{chan} = 500$
$r_{\text{cell}} = 0.5$km	$\text{PL}_{\text{dB}} = 137.74 + 30.\log_{10}(d), d$[km]	$n_{\text{step}} = 20$

TABLE II: System model and algorithm settings.

information amount of the three sectors. In the remainder of the paper, ARAP is introduced just for S_1; adaptation for the global system is easily deduced from adaptation of each sector.

ARAP is applied in S_1 for a given location of $\mathbf{d}_1$. *GMI* of all allocation modes are first averaged on various communication contexts (fading, shadowing, random mobility of $\mathbf{d}_2$ and $\mathbf{d}_3$), and then weighted by the power budget of allocation modes. The result is identified by $\widehat{GMI}_{\mathbf{d}_1}$. After that, ARAP selects from a subset $\mathscr{K}$ of modes the one maximizing $\widehat{GMI}_{\mathbf{d}_1}$. This optimal mode is designed by $\mathscr{M}^{\mathbf{d}_1}_{\mathscr{K}}$. Subset $\mathscr{K}$ is chosen among $\{\Omega_{\text{clas}}, \Omega_{\text{adv}}, \Omega_{\text{all}}\}$, which are respectively subsets of all classical, all *Advanced* and all investigated modes.

A $n_{\text{step}} \times n_{\text{step}}$ grid parcels out each sector. $\mathscr{M}^{\mathbf{d}_1}_{\mathscr{K}}$ is selected for all positions of $\mathbf{d}_1$ on its grid. Figure 6 illustrates the algorithm steps, while simulation results are shown in Section V.

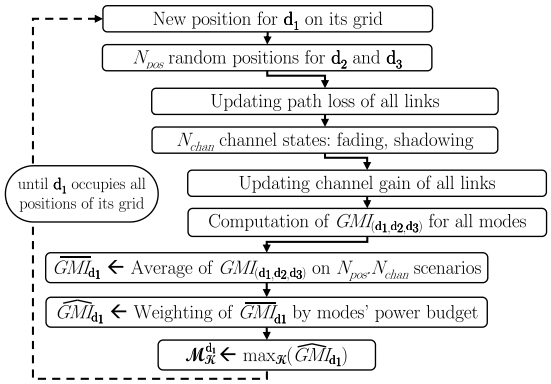

Fig. 6: Description of the algorithm for RRM adaptation

V. Simulation Results

In this section we show our simulation results for both proposed and classical allocation modes presented in Section III. Performance are compared in terms of *GMI* and power consumption. Two scenarios are considered. First scenario (see Fig. 7–8): $\mathbf{d}_1$'s mobility is constrained to the axis ($\mathbf{s}_1$–$\mathbf{r}_1$), while in sectors S_2 and S_3, destinations move randomly. Second scenario (see Fig. 9a and 9b): destination $\mathbf{d}_1$ occupies alternately all positions of its grid, and for each position of this grid, destinations $\mathbf{d}_2$ and $\mathbf{d}_3$ are randomly mobile. Performance with both OAF and ODF cooperative protocols are evaluated. With OAF protocol, the amplification gain is defined such that transmitted signal power equals P_{r_i}; while with ODF protocol, relays are assumed to decode their signal without error. System model and algorithm settings adopted in our numerical results are summarized in Table II.

On Figures 7 (OAF) and 8 (ODF) we plot the evolution of $\widehat{GMI}_{\mathbf{d}_1}$ with the increasing distance between $\mathbf{s}_1$ and $\mathbf{d}_1$. Dotted dashed and solid curves represent respectively results for *Classic*$_1$ and *Advanced* allocation modes. Results for *Classic*$_2$ modes are not shown, since both *Classic*$_1$ and *Advanced* modes outperform *Classic*$_2$ ones in all scenarios. We represent results belonging to each family of modes with a dedicated marker and a specific color: NNN (red curve, no marker), CNN (green curve, upward-pointing triangle), NCN (blue curve, downward-pointing triangle), CCN (magenta curve, circle), NCC (gray curve, plus sign) and CCC (black curve, five-pointed star). Results for families NNC and CNC are identical respectively to those of families NCN and CCN (by design symmetry) and are thus not shown. Mobility of $\mathbf{d}_1$ does not impact the amount of mutual information of sectors S_2 and S_3. As expected due to path loss attenuation, the farer is $\mathbf{d}_1$ from $\mathbf{s}_1$, the lower is mutual information amount of S_1, and thus $\widehat{GMI}_{\mathbf{d}_1}$. However, when S_1 plans cooperation (CNN, CCN, CCC families), $\widehat{GMI}_{\mathbf{d}_1}$ improves close to $\mathbf{r}_1$ (dist($\mathbf{s}_1$,$\mathbf{d}_1$)=0.33km). With our assumptions, ODF protocol cancels interference while OAF protocol amplifies interference. $\widehat{GMI}_{\mathbf{d}_1}$ enhancements in the vicinity of $\mathbf{r}_1$ are therefore bigger with ODF protocol (Fig. 8) than with OAF (Fig. 7). When $\mathbf{d}_1$ is out of reach of $\mathbf{r}_1$ (dist($\mathbf{r}_1$,$\mathbf{d}_1$)$\gtrsim$0.11km), NNN_{C1} allocation mode (also used as NNN_{A}) outperforms other modes, for both OAF and ODF.

Eventually, we observe that our proposed *Advanced* allocation modes outperform Classic modes both in terms of power consumption and efficiency of inter-site resource allocation. We further observe how, the smaller is the number of sectors in which cooperation is activated, the higher is the $\widehat{GMI}_{\mathbf{d}_1}$.

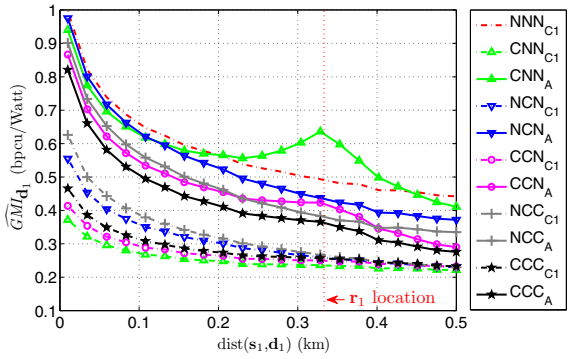

Fig. 7: $\widehat{GMI}_{\mathbf{d}_1}$ variations along ($\mathbf{s}_1$–$\mathbf{r}_1$) axis, OAF protocol

On Figures 9a (for OAF) and 9b (for ODF) we show for each position of $\mathbf{d}_1$ in S_1 which allocation family maximizes $\widehat{GMI}_{\mathbf{d}_1}$ ($\mathscr{M}^{\mathbf{d}_1}_{\Omega_{\text{all}}}$). Adaptation is done among all investigated allocation modes (Ω_{all}). On these figures, each position of the grid is marked by a circle, filled with the color assigned to $\mathscr{M}^{\mathbf{d}_1}_{\Omega_{\text{all}}}$ family of allocation modes. Color assignments are the followings: NNN (red with black edge), CNN (green), NCN (blue) and NNC (white with black edge). Other modes families

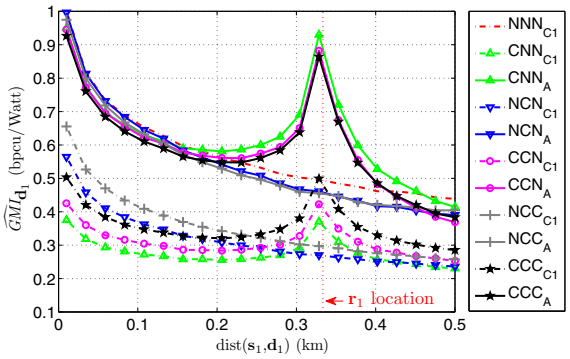

Fig. 8: $\widehat{GMI}_{\mathbf{d}_1}$ variations along ($\mathbf{s}_1$–$\mathbf{r}_1$) axis, ODF protocol

are never optimal and are consequently not shown on these figures for more readability.

ARAP suggests to plan cooperation in at most one sector. Actually, families NNN, CNN, NCN and NNC cover all positions of the grid. Figures 9a and 9b confirm remarks of Figures 7 and 8: family CNN (green) is optimal in the vicinity of $\mathbf{r}_1$, while elsewhere family NNN (red) is the best. There are nevertheless two exceptions: the highest and the lowest areas of S_1, colored respectively in white and blue. When $\mathbf{d}_1$ is placed on the white area for instance, $\mathbf{d}_1$ is sufficiently remote from $\mathbf{r}_3$, so that sector S_3 could plan cooperation (NNC family) without interfering too much with $\mathbf{d}_1$. Inter-sector interference caused by $\mathbf{r}_3$ on $\mathbf{d}_1$ is then lower than enhancements of mutual information amount in sector S_3. By symmetry, NCN family is optimal when $\mathbf{d}_1$ is sufficiently apart from $\mathbf{r}_2$. Due to our assumptions on cooperative protocols, relay activation areas are larger with ODF (Fig. 9b) than with OAF (Fig. 9a).

Results obtained with adaptation on Ω_{clas} (all classical modes) are not shown: NNN family is everywhere optimal (all in red). There is a single exception with ODF: a unique black circle (family CCC) close to $\mathbf{r}_1$. On the other hand, if the RRM adaptation is restricted to Ω_{adv} (all *Advanced* modes), then results are exactly the same as those on Figures 9a (OAF) and 9b (ODF). Therefore, *Advanced* modes outperform everywhere classical modes. Indeed, optimal adaptation can be restricted to Ω_{adv}, without degradation.

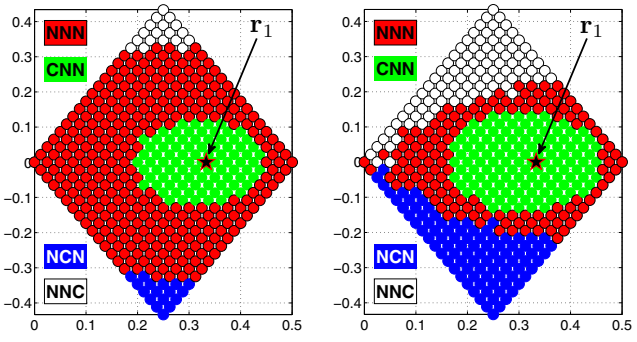

(a) OAF protocol (b) ODF protocol

Fig. 9: Adaptive Resource Allocation Process with set Ω_{all}

VI. Conclusions

This paper proposes novel efficient inter-site resource allocation modes for two hops cooperative communication systems where relays are half-duplex per chunk. We show by numerical evaluation that the advantages of the proposed solutions are twofold. First, overall power consumption is lowered. Second, by protecting relays from inter-site interference, cooperative transmissions further permit to increase the global amount of mutual information in all investigated communication scenarios. These results are benchmarked by our simulation results. In this paper we also evaluate the performance of an ideal inter-site resource allocation mechanism which jointly selects the allocation modes that maximize the global mutual information for the given instantaneous channel instance and location of users. We observe that while border cell users do not cooperate (cooperation does not help in extending site coverage), the area of the cell in which cooperation improves performance is notably extended. In this paper, we target to enlarge the areas in cells where cooperation ameliorates performance while limiting the interference caused to neighbor sites. Further work will focus on the improvement of cooperation effectiveness for cell-edge users which suffer the most from inter-site interference.

Acknowledgments

This work has been performed in the framework of the FP7 project ROCKET IST-215282 STP, which is funded by the European Community.

References

[1] Y. Xiang, J. Luo and C. Hartmann, "Inter-cell interference mitigation through flexible resource reuse in OFDMA based communication networks," *Proc. European Wireless 2007*, pp. 1–7, Apr. 2007.

[2] X. Fan, S. Chen and X. Zhang, "An inter-cell interference coordination technique based on users' ratio and multi-level frequency allocations," *IEEE WiCom 2007*, pp. 799–802, Sep. 2007.

[3] D. Tse and P. Viswanath, "Fundamentals of wireless communication," Cambridge University Press, May 2005.

[4] K. Gomadam, V.R. Cadambe and S.A. Jafar, "Approaching the capacity of wireless networks through distributed interference alignment," *IEEE GLOBECOM 2008*, pp. 1–6, Nov. 2008.

[5] S.M. Perlaza, M. Debbah, S. Lasaulce and J.-M. Chaufray, "Opportunistic interference alignment in MIMO interference channels," *IEEE PIMRC 2008*, pp. 1–5, Sep. 2008.

[6] E. Calvanese Strinati, S. Yang and J.-C. Belfiore, "Adaptive modulation and coding for hybrid cooperative networks," *IEEE ICC 2007*, pp. 4191–4195, Jun. 2007.

[7] S. Boyd and L. Vandenberghe, "Convex optimization," Cambridge University Press, Mar. 2004.

[8] M. Chiang, C.W. Tan, D.P. Palomar, D. O'Neill and D. Julian, "Power control by geometric programming," *IEEE Trans. Wireless Comm.*, vol. 6, no. 7, pp. 2640-2651, Jul. 2007.

[9] T.M. Cover and J.A. Thomas, "Elements of information theory," Wiley-Interscience, 2nd Edition, Jul. 2006.

[10] D. Gesbert, S.G. Kiani, A. Gjendemsjo and G.E. Oein, "Adaptation, coordination and distributed resource allocation in interference-limited wireless networks," *IEEE Proc.*, vol. 95, no. 12, pp. 2393–2409, Dec. 2007.

[11] X. Cai and G. Giannakis, "A two-dimensional channel simulation model for shadowing processes," *IEEE Trans. Vehicular Technology*, vol. 52, no. 6, pp. 1558–1567, Nov. 2003.

[12] Z. Yong, L. Jun, X. Youyun and C. Yueming, "An adaptive non-orthogonal cooperation scheme based on channel quality information," *IEEE WiCom 2007*, pp. 988–991, Sep. 2007.